Structural Geology (The Journal of the Tectonic Research Group of Japan), No. 45, 47–64, 2001

Genesis of Okinawa Trough and thrust development within accretionary prism by means of 2D finite element method

Handi Lu* and Daigoro Hayashi**

Abstract : The Okinawa Trough is a back-arc basin opened by crustal extension within the Eurasia plate. Several two-dimensional (2D) finite element models are presented to simulate the stress field and fault development in the upper continental lithosphere of the Eurasia plate. Linear elastic rheology with failure criterion under plane strain condition is adopted. Two types of displacement boundary condition are considered in the numerical model. The spreading displacement is applied along the crustal bottom beneath the Okinawa Trough. The convergence displacement is subjected along the upper side of the Philippine Sea (PHS) plate. From the simulated results, the spreading displacement along the crustal bottom generates normal faults in the trough, which finally leads to the formation of the Okinawa Trough. The subduction of the PHS plate causes the thrust development within the accretionary prism of the Eurasia plate. The results from our numerical experiment are in agreement with the earthquake focal mechanism in the study area.

Key words : *Okinawa Trough, finite element method, spreading displacement, convergence displacement, fault development, accretionary prism*

Introduction

The Ryukyu trench-arc-back-arc system, Okinawa Trough, Ryukyu Arc and Ryukyu Trench, is an active continental margin between the Eurasia plate and the Philippine Sea (PHS) plate (Fig. 1). Numerous recent observations have contributed to the genesis of the Okinawa Trough (Herman et al., 1978 ; Lee et al., 1980 ; Kimura, 1985 ; Letouzey & Kimura, 1985 ; Sibuet et al., 1987 ; Miki, 1995 ; Park et al., 1998).

Based on the kinematics of the Eurasia plate and the PHS plate (Seno, 1977), several 2D finite element models with different rheologies and boundary conditions were proposed. Huchon et al. (1986) presented a 2D viscous finite element model for simulating a rigid body (the Luzon Arc) indenting into a rigid-plastic material (the Chinese continental margin). Viallon et al. (1986) gave a 2D finite element model of the Okinawa Trough with an elasto-plastic behavior, and showed that the opening of the Okinawa Trough behind the Ryukyu Trench could be explained by a retreating trench model with lateral anchoring due to the collision in Taiwan. Hu et al. (1996) used a 2D finite element model of plane stress with elastic and elasto-plastic rheologies to analyze the relationship between kinematics of convergence, deformation and stress distribution in the present Taiwan collision occurring between the Ryukyu and Luzon subduction zones.

In this paper we aim to analyze the genesis of the back-arc trough and thrust development within the accretionary prism (tip of the Eurasia plate) by means of 2D finite element method (FEM) as follows. (1) Based on the P-wave structural profile modified from the works of Ludwing et al. (1973), Kimura (1983), Iwasaki et al. (1990), Hirata et al. (1991), Kodaira et al. (1996) and Park et al. (1998), the finite element grid of the models are produced. (2) 2D and semi-3D stress fields of the models are simulated when several different combinations of the spreading displacement along the crustal bottom beneath the Okinawa Trough and the convergence dis-

Received 12 March 2001 ; accepted 4 July 2001
* Graduate School of Engineering and Science, University of the Ryukyus, Nishihara, Okinawa 903–0213
** Department of Physics and Earth Sciences, University of the Ryukyus, Nishihara, Okinawa 903–0213

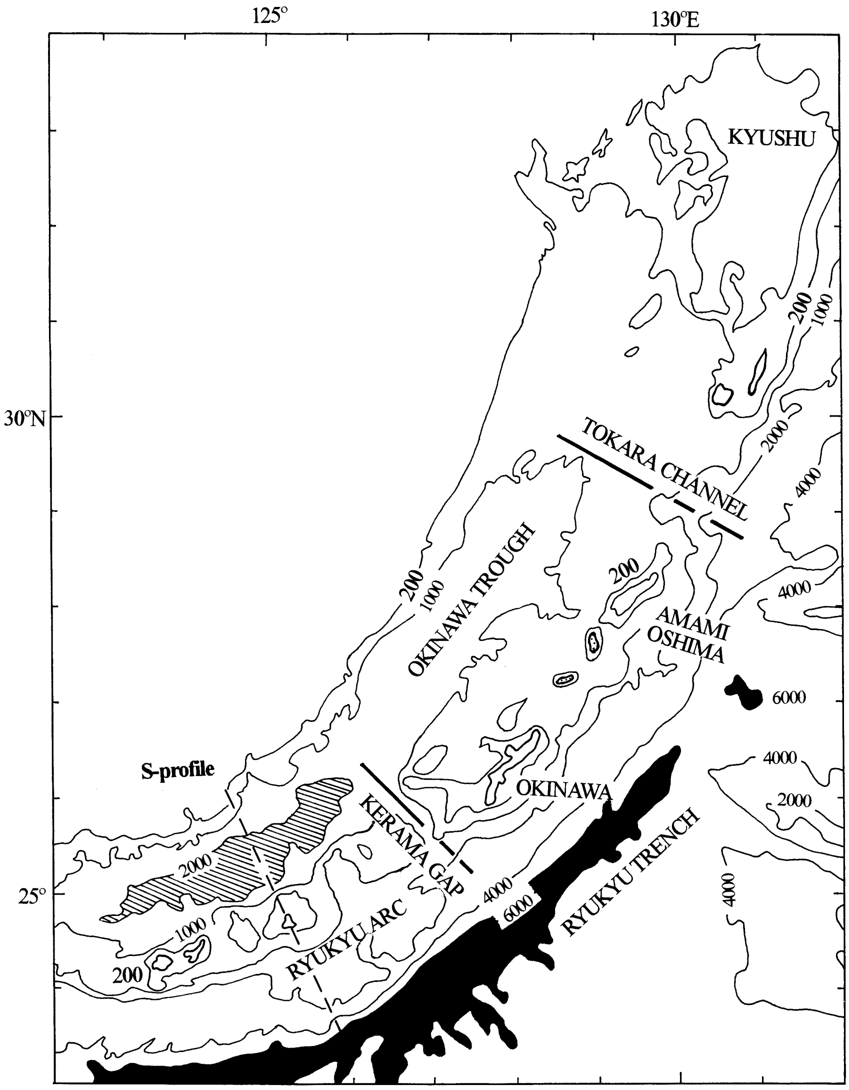

Fig. 1 Index map showing the Okinawa Trough, Ryukyu Island Arc and Ryukyu Trench slightly modified from Kodaira et al. (1996). Numerical analysis along southern profile (S-profile) is carried out.

placement along the subduction slope of the PHS plate are subjected as the boundary condition. (3) The development of normal fault in the trough and thrust fault within the accretionary prism of the Eurasia plate is analyzed according to the Coulomb-Mohr criterion. (4) The simulated results are compared with the earthquake focal mechanism in the study area.

Tectonic setting

1. Okinawa Trough, Ryukyu Arc, Ryukyu Trench

The Ryukyu Arc and the Okinawa Trough are typical examples of island arc and back-arc basin which construct the continental plate margin. The Okinawa Trough is a back-arc spreading zone between the East China Sea and the Ryukyu Islands, formed by extension within continental lithosphere behind the Ryukyu Trench-Arc system as shown in Fig. 2 (Letouzey & Kimura, 1985). The Okinawa Trough extends from southwest Kyushu in the northeast to Taiwan in the southwest. It is only 60〜100 km wide in the south and reaches up to 230 km wide in the north. Its maximum water depth is about 2300 m in the south and progressively decreases to 200 m in the north.

The exact timing of the trough opening is always under argument. Although there is a consensus about the last two phases of extension occurring in the Okinawa Trough since 2 Ma, there is a large controversy about the age of the early rifting phase (Sibuet et al., 1998). Seismic profiles and geological observation in the trough indicate that the rifting started in the late Miocene (Herman et al., 1978 ; Lee et al., 1980 ; Letouzey & Kimura, 1986 ; Sibuet et al., 1987).

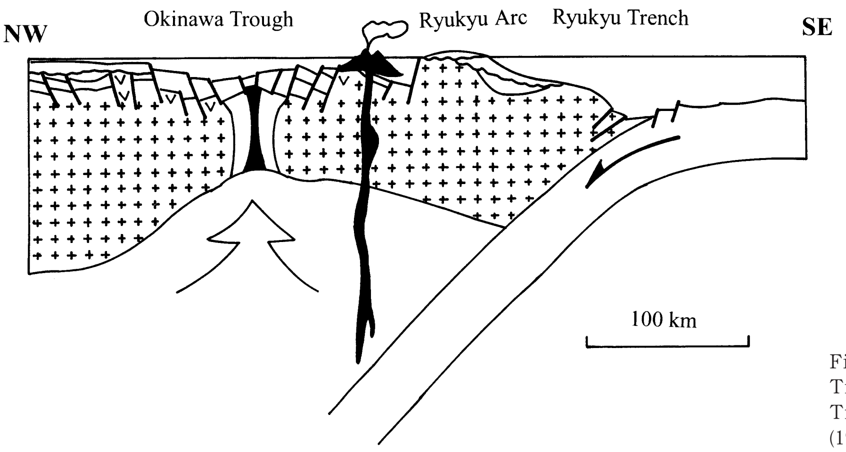

Fig. 2 Idealized cross section of the Okinawa Trough, Ryukyu Island Arc and Ryukyu Trench modified from Letouzey and Kimura (1985).

Kimura (1985) suggested that in the center of the southern Okinawa Trough spreading initiated in the early Pleistocene (about 1.9 Ma ago). Average half-spreading rate has been up to 2 cm/y. The northern Okinawa Trough is in a beginning stage to rift (Letouzey & Kimura, 1985 ; Kimura, 1985). Miki (1995) gave a two-phase opening model for the origin of the Okinawa Trough on the basis of paleomagnetic and geochronological research, and suggested that the first phase would be between 10 Ma and 6 Ma, and the second phase at about 1 Ma.

The Ryukyu Arc extends from Taiwan to south Kyushu as shown in Fig. 3 (Letouzey & Kimura, 1985). It is an elevated ridge marked by two parallel chains comprising more than 100 islands. Islands along the inner arc are volcanoes of Quaternary age, whereas those along the outer arc are non-volcanic outcrops (Iwasaki et al., 1990). The Ryukyu Arc is divided into three segments by the Tokara Channel and the Kerama Gap, which are considered to be left-lateral strike-slip faults (Wageman et al., 1970 ; Kobayashi, 1985).

The Ryukyu Trench is usually regarded to be the boundary between the Eurasia plate and the PHS plate. The maximum water depth of the trench is more than 7000 m near the Okinawa Island while most parts of the trench are not

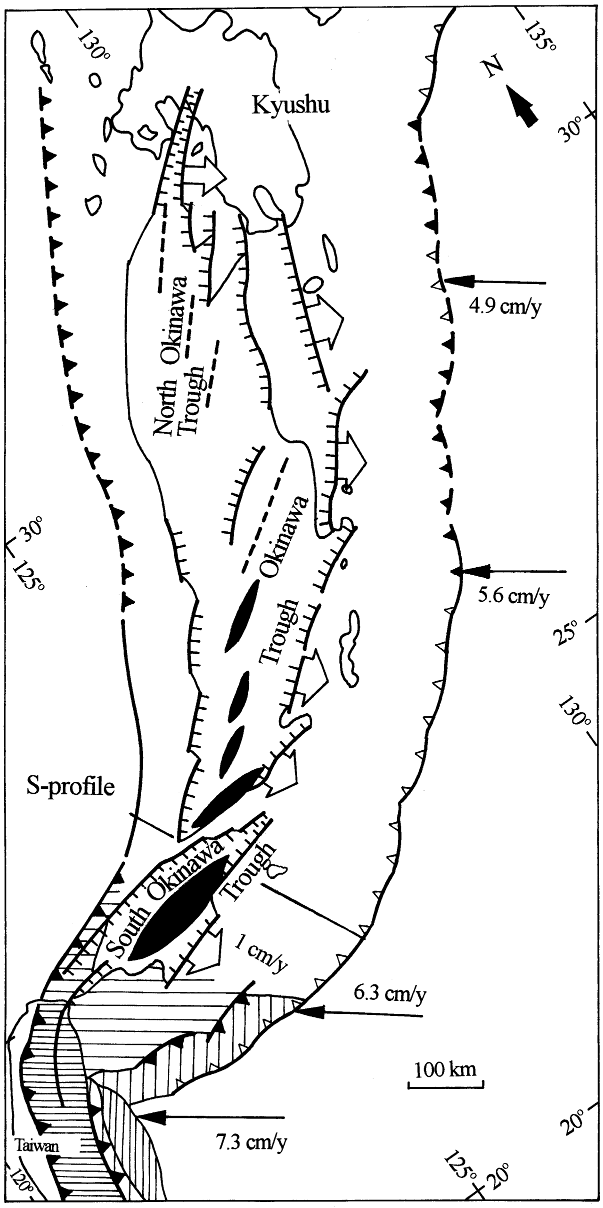

Fig. 3 Tectonic index map of the Taiwan-Ryukyu-Okinawa region modified from Letouzey and Kimura (1985). Arrows at the trench show the convergence of the Philippine Sea plate with respect to the Eurasia plate, based on the model of Seno (1977). Arrows at the Okinawa Trough show the spreading of the Okinawa Trough.

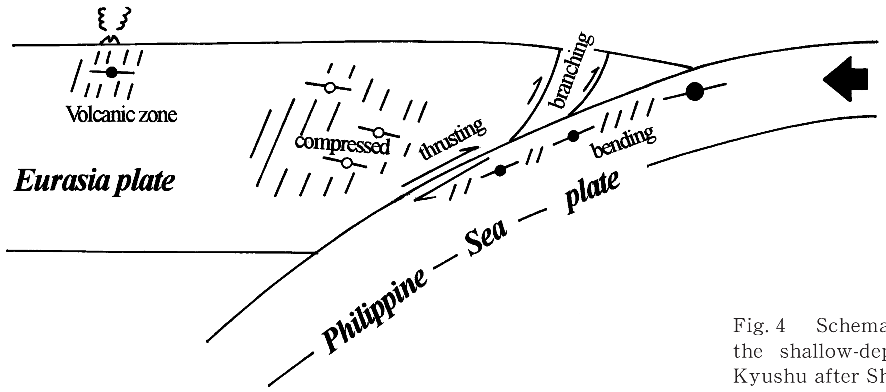

Fig. 4 Schematic illustration of the focal mechanism of the shallow-depth earthquakes from Taiwan to south Kyushu after Shiono et al. (1980).

deeper than 6500 m. The trench becomes shallower and broader towards the north, where the trench is with a depth of about 5500 m.

2. Earthquake focal mechanism

Tectonic features of the Kyushu-Ryukyu Arc were investigated in detail by Shiono et al. (1980), on the basis of seismicity and focal mechanism solution of shallow to intermediate depth earthquakes with magnitudes around and greater than 5.0. The focal mechanism of the shallow-depth earthquakes is summarized, as a schematic illustration in Fig. 4 (Shiono et al., 1980). From the focal mechanism, stress is tensional in the Okinawa Trough, and thrust faults develop within the accretionary prism as the PHS plate subducts beneath the Eurasia plate.

Finite element modeling

1. Model geometry

The southern profile (S-profile), a seismic P-wave structural section, has been constructed on the basis of the works of Ludwing et al. (1973), Kimura (1983), Hirata et al. (1991) and Park et al. (1998). S-profile is about 320 km long with a depth of about 18 km. (Fig. 5). The sedimentary wedge of the continental crust consists of three layers, whose P-wave velocities are 1.8～1.9, 2.0～3.6 and 4.5 km/s at the top of each layer as shown in Fig. 5. The 1.8～1.9 and 2.0～3.6 km/s layers are assumed to be composed of sandstone, while the layer 4.5 km/s is considered to be composed of limestone. The P-wave velocities of granite layer are 6.2～6.4 and 7.0～7.2 km/s. The Moho depth is deduced to be about 18 km beneath the southern Okinawa Trough. The descending velocity of the PHS plate beneath the Eurasia plate is assumed to be 6.3 cm/y in the southern section (Fig. 3). The angle between the strike of S-profile and the convergence direction of the PHS plate is 26°. The angle between the striking of S-profile and the spreading direction under the trough is 9°. The dip of the subduction slope of the PHS plate is 19° to the horizon (Fig. 5).

2. Finite element grid

The finite element grid of model S is 320 km long and 18 km deep as shown in Fig. 6. It is composed of 624 nodes and 1041 triangular elements. In the grid of model S, different kinds of line (thin, thick and intermediate) indicate sandstone, limestone and granite. The grid of models S1, S2 and S3 is the same as model S, but their two types of displacement boundary condition are different from each other (Fig. 6, Table 2).

3. Physical properties

The continental crust of the Eurasia plate is simplified to be composed of sandstone, limestone and granite from top to bottom as a three-layered elastic continuum. Since we have adopted the elastic rheology in the simulation, physical properties of sandstone, limestone and granite are listed in Table 1.

4. Boundary conditions

Two types of displacement boundary condition but no tectonic force are imposed in finite element models. Neither trench suction force nor overriding plate resistance force is considered in numerical model. This point is also the speciality of our numerical experiment. The spreading displacement is applied along the crustal bottom beneath the trough to represent the spreading of the Okinawa Trough. Since the PHS plate subducts beneath the Eurasia plate, the convergence displacement is subjected to the upper side of the descending plate along the

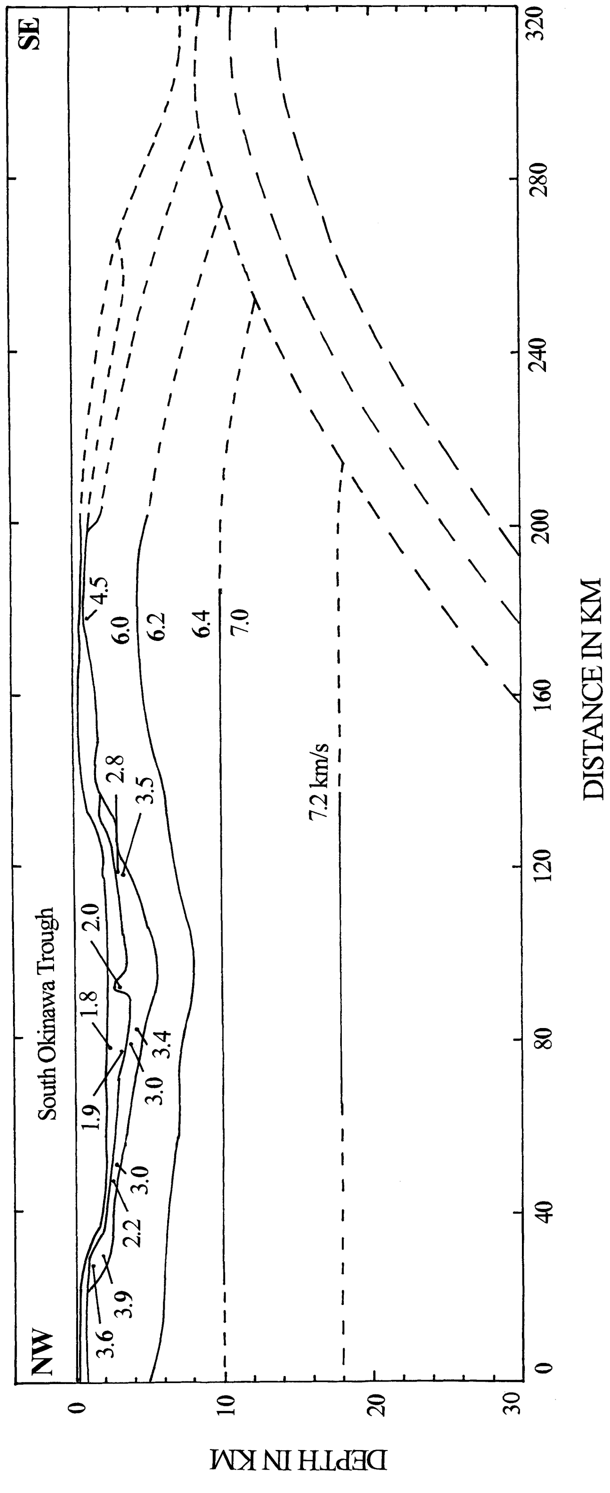

Fig. 5 P-wave velocity structure of the S-profile modified from the works of Kimura (1983), Hirata et al. (1991) and Park et al. (1998). Vertical exaggeration is taken as about 15 : 2. Dashed lines are extrapolations of the interfaces obtained by the ocean bottom seismometer (OBS) data.

subduction slope.

The boundary conditions of model S are in detail as follows (Table 2). The basal nodes on the crustal bottom (BG) are constrained to zero vertical displacement but are free horizontally, though the negative and positive spreading displacements are given along the crustal bottom under the trough. The nodes at left edge (AB) of the lithosphere are constrained to zero horizontal displacement but are free vertically. Node B is fixed. The nodes of the overriding plate on the subduction slope are applied with the convergence displacement. The convergence displacement decreases gradually from the node (504 m) at the shallow place to that at the deep place (168 m) on the subduction slope, and the convergence displacement decrement is 28 m.

5. Finite element method

Since the stretch of the Okinawa Trough, Ryukyu Arc and Ryukyu Trench is more than 1000 km and approximately perpendicular to the convergence direction of the PHS plate, linear elastic rheology with plane strain condition is applied to analyze the stress field of the upper lithosphere of the Eurasia plate. The finite element modeling is carried out with the linear elastic elas.f code (developed by D. Hayashi). Gravitational body forces are included in the models.

All the finite element models are in 2D elastic state under the plane strain condition. Since 2D stress fields of the numerical models are simulated with the elas. f code, the third principal stress σ^*, which acts perpendicularly to the section plane, can be obtained from the theory of plane strain as

$$\sigma^* = \nu \cdot (\sigma_1 + \sigma_2) \qquad (1)$$

where ν is Poisson's ratio (Timoshenko & Goodier, 1970 ; Hayashi & Kazaki, 1972). Since the values of σ_1, σ_2 and σ^* of each finite element have been calculated, we can define which principal stress (σ_1, σ_2, σ^*) is the maximum, intermediate and minimum principal stress. The semi-3D stress field of each model is envisaged with the newly obtained principal stresses σ_1, σ_2 and σ_3.

As the semi-3D stress field of each model is available, it is possible to describe in which finite element, fault will develop according to the Coulomb-Mohr criterion. The criterion is expressed on a linear relationship between the shear stress τ and the normal stress σ_n as

$$\tau = c + \sigma_n \cdot \tan\phi \qquad (2)$$

where c is the cohesion strength and ϕ is the internal friction angle as shown in Fig. 7

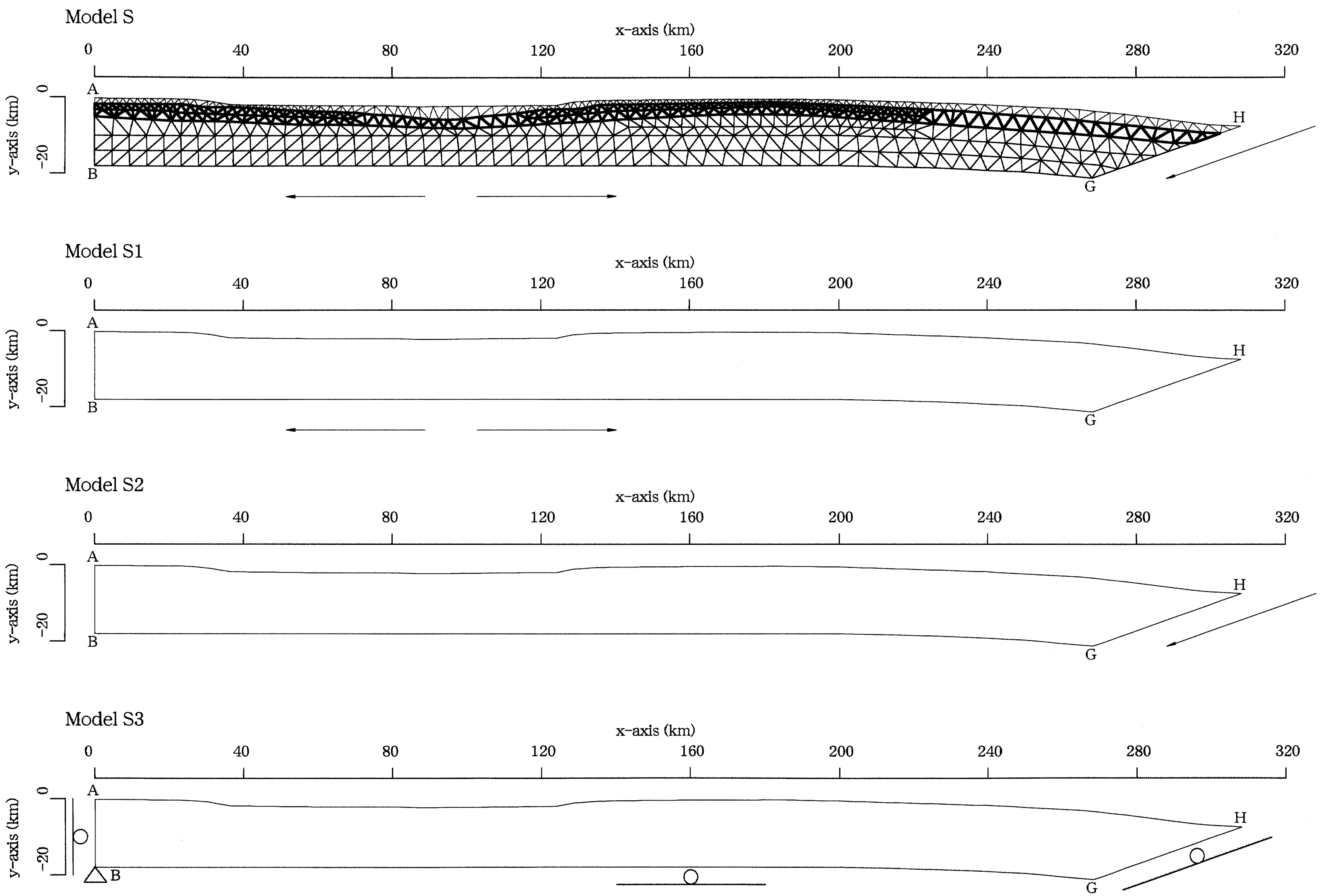

Fig. 6 Finite element grid of model S. The grid is composed of 624 nodes and 1041 triangular elements. Thin, thick and intermediate lines indicate sandstone, limestone and granite. Physical properties are listed in Table 1. Lines with arrow represent the two types of displacement boundary condition (see text and Table 2). The grid of models S1, S2 and S3 is the same as model S.

Table 2 Two types of displacement boundary condition subjected in finite element models.

	Model	Spreading displacement (m)	Convergence displacement (m) (Decrement (m))
Experiment I	S	80	504 ~ 168 (28)
	S1	80	0
	S2	0	504 ~ 168 (28)
	S3	0	0
Experiment II	S-A	20	504 ~ 168 (28)
	S-B	40	504 ~ 168 (28)
	S-C	80	504 ~ 168 (28)
	S-D	200	504 ~ 168 (28)
Experiment III	S-I	80	126 ~ 42 (7)
	S-II	80	252 ~ 84 (14)
	S-III	80	504 ~ 168 (28)
	S-IV	80	1008 ~ 336 (56)

Table 1 Physical properties applied for sandstone, limestone and granite.

	Sandstone	Limestone	Granite
Young's modulus (GPa)	45.7	63.3	77.4
Poisson's ratio	0.234	0.260	0.336
Densities (kg/m^3)	2543	2656	2644
Cohesion (MPa)	35	36	23
Internal friction coefficient	0.90	0.70	1.60
Internal friction angle (deg.)	42°	35°	56°

Data are from Clark, 1966

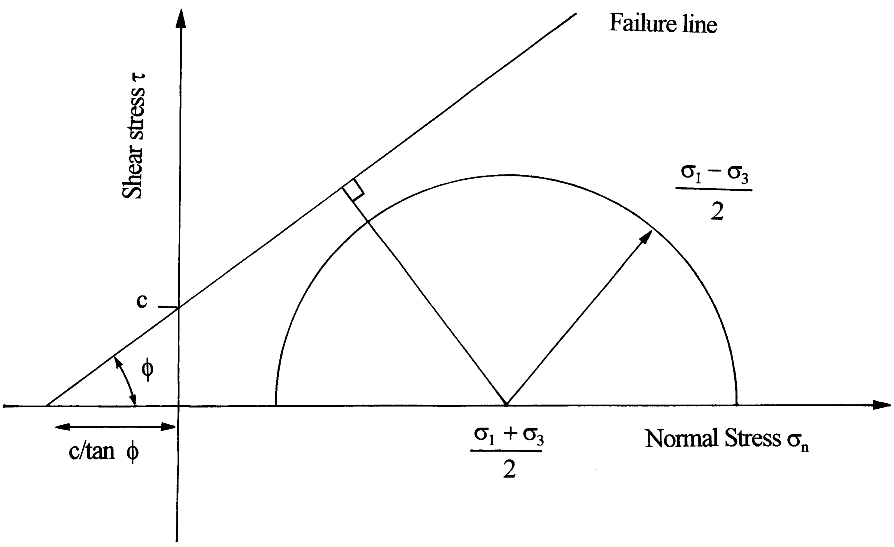

Fig. 7 Linear Coulomb-Mohr criterion demonstrating the concept of proximity to failure after Melosh and Williams (1989).

(Melosh & Williams, 1989) and listed in Table 1 (Clark, 1966). Failure develops when the Mohr's stress circle touches the Coulomb-Mohr failure envelope. This takes place when the radius of the Mohr's stress circle, $(\sigma_1-\sigma_3)/2$, is equal to or greater than the perpendicular distance from the center of the circle, $(\sigma_1+\sigma_3)/2$, to the failure envelope.

The proximity to failure P_f is calculated for each finite element of the models using the following equations (Melosh & Williams, 1989).

$$((\sigma_1-\sigma_3)/2)_{\text{failure}} = c \cdot \cos\phi + ((\sigma_1+\sigma_3)/2) \cdot \sin\phi \quad (3)$$

$$P_f = ((\sigma_1-\sigma_3)/2)/((\sigma_1-\sigma_3)/2)_{\text{failure}} \quad (4)$$

We can evaluate whether faulting occurs in certain finite element according to the value of parameter P_f. If the value of P_f is less than 1.0, the Mohr's stress circle is inside the failure envelop and no fault develops, but faulting occurs whenever P_f exceeds 1.0. Thus the parameter P_f

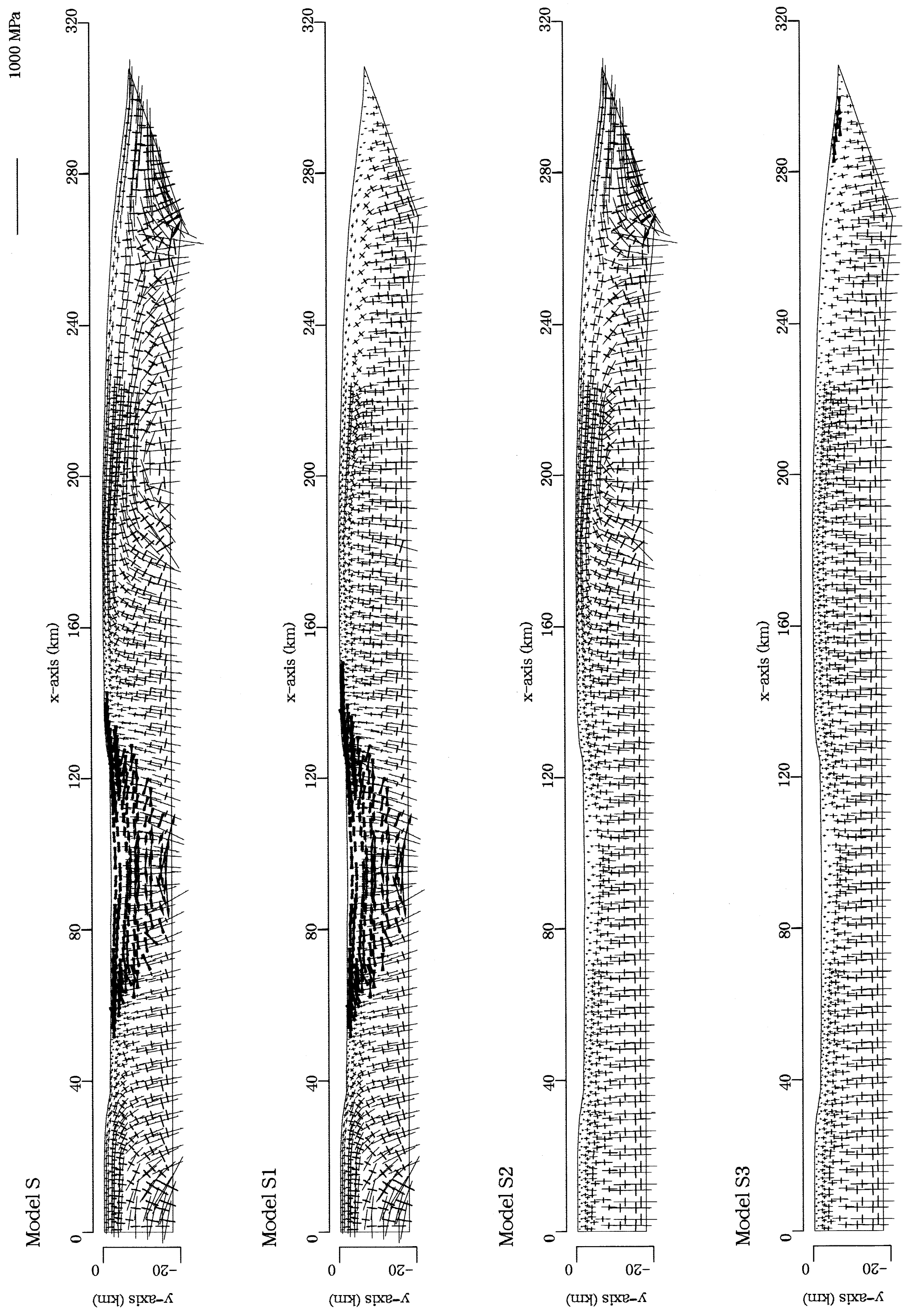

Fig. 8 Magnitude and orientation of the principal stresses in the semi-3D stress fields of models S, S1, S2 and S3. Straight lines represent compression, and lines with arrow represent tension. Note that the boundary condition is different in the four models.

is taken as an indicator to define whether the fault develops or not.

Modeling results

1. Stress field

The semi-3D stress fields of models S, S1, S2 and S3 are simulated as shown in Fig. 8. σ_1 and σ_3 represent the maximum and minimum principal stresses, and compression is taken as positive.

The spreading displacement of 80 m and the convergence displacement varying from 504 m to 168 m are subjected to model S as the boundary condition (Table 2). The main feature of the stress field of model S is that σ_3 is tensional in the southern Okinawa Trough and that compressive σ_1 is nearly horizontal within the accretionary prism of the Eurasia plate. In the southern Okinawa Trough, compressive σ_1 is nearly vertical while tensional σ_3 is nearly horizontal. In the southern Ryukyu Arc, compressive σ_1 is nearly horizontal while compressive σ_3 is nearly vertical at the shallow place (0〜12 km deep). However compressive σ_1 and σ_3 are inclined at the deep place (12〜26 km deep). Within the accretionary prism, compressive σ_1 is nearly horizontal and compressive σ_3 is nearly vertical. σ_1 is compressive and nearly vertical in the trough while compressive σ_1 is nearly horizontal within the accretionary prism. The maximum values of compressive σ_1 and σ_3 are 854 MPa and 304 MPa, respectively. The absolute maximum value of tensional σ_3 is 943 MPa.

The spreading displacement of 80 m but no convergence displacement is applied as the boundary condition in model S1 (Table 2). The stress distribution of model S1 is similar to that of model S in the trough, but is different from model S within the accretionary prism of the Eurasia plate where compressive σ_1 is roughly vertical in model S1. The convergence displacement varying from 504 m to 168 m is loaded as the boundary condition in model S2 (Table 2). In the trough, the stress field of model S2 is different from model S since σ_3 is compressive in model S2. Within the accretionary prism of the Eurasia plate, the stress field of model S2 is similar to model S. Neither the spreading displacement nor the convergence displacement is subjected to model S3 as the boundary condition (Table 2). The stress distribution of model S3 is definitely different from model S in the trough and within the accretionary prism. In model S3, σ_3 is compressive in the trough and compressive σ_1 is nearly vertical in the accretionary prism of the Eurasia plate.

2. Influence of displacement boundary condition to stress field

The stress fields of models S, S1, S2 and S3 show different features from each other. In the trough, σ_3 is tensional in models S and S1 while the spreading displacement of 80 m is applied as the boundary condition. However no tensional stress occurs in models S2 and S3 with no spreading displacement subjected. The stress fields of models S2 and S3 are similar to each other in the trough, though their convergence displacement boundary conditions are different. The stress field of model S1 is similar to model S in the trough, whereas their convergence displacement boundary conditions are different. Thus the spreading displacement loaded as the boundary condition raises up tension in the trough. The convergence displacement subjected as the boundary condition hardly affects the stress distribution in the trough.

Within the accretionary prism of the Eurasia plate, compressive σ_1 is nearly horizontal in models S and S2 while the convergence displacement varying from 504 m to 168 m is loaded as the boundary condition. However compressive σ_1 is nearly vertical within the accretionary prism in models S1 and S3 as zero convergence displacement is applied. The stress field of model S is similar to model S2 within the accretionary prism, though their spreading displacement boundary conditions are different. The stress field of model S1 is similar to model S 3 within the accretionary prism, whereas their spreading displacement boundary conditions are different. Thus the convergence displacement generates horizontal compressive σ_1 within the accretionary prism of the Eurasia plate. The spreading displacement has little effect on the stress distribution within the accretionary prism.

3. Influence of displacement boundary condition to fault development

The style of fault development is different in models S, S1, S2 and S3 as shown in Fig. 9. In the

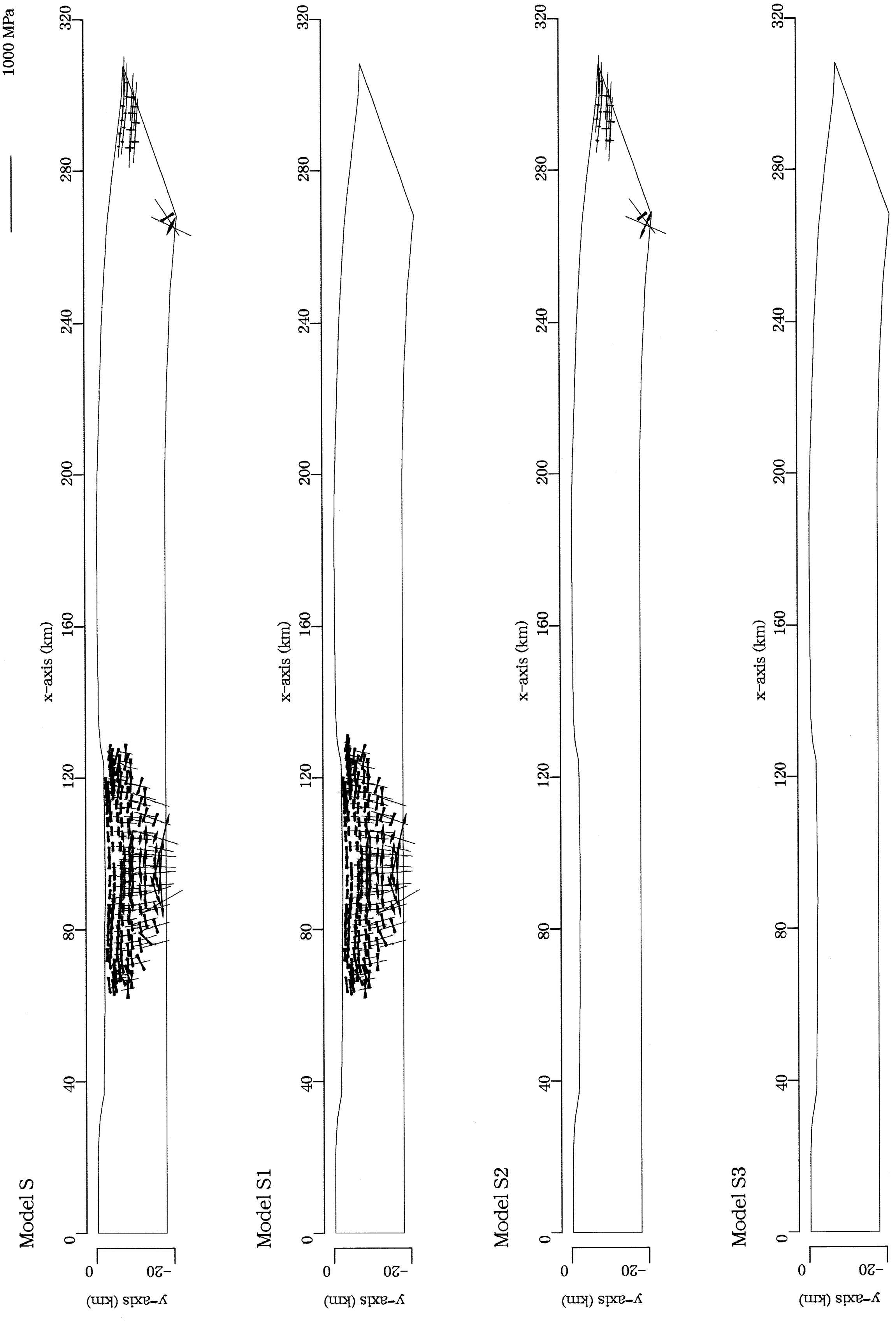

Fig. 9 Fault development in models S, S1, S2 and S3. The maximum and minimum principal stresses are illustrated just for the finite element with Pf > 1.0 in the four models. Straight lines represent compression, and lines with arrow represent tension.

trough, normal faults develop in models S and S 1 with the spreading displacement subjected as the boundary condition. On the other hand no normal fault develops in models S2 and S3 as zero spreading displacement is applied. Within the accretionary prism of the Eurasia plate, thrust faults develop in models S and S2 in which the convergence displacement varying from 504 m to 168 m is loaded. However no thrust fault develops in models S1 and S3 as zero convergence displacement is subjected. Thus the spreading displacement generates normal faults in the trough and it hardly affects thrust development within the accretionary prism. The convergence displacement causes thrust development within the accretionary prism of the Eurasia plate and it has little effect on the fault development in the Okinawa Trough.

Discussion

All the finite element models here are assumed to be elastic in the simulation. The elastic assumption is based on the theory of plate tectonics (Turcotte & Schubert, 1982). The continental lithosphere is considered to be internally rigid. The rigidity of the lithosphere allows the plates to transmit elastic stresses during geologic intervals. Generally the continental lithosphere has a thickness of more than 100 km, though the thickness of our numerical models is less than 20 km in the Eurasia continental plate. Although the entire lithosphere is not effective in transmitting elastic stresses, the upper half of it is sufficiently rigid. This fraction of the lithosphere is referred to as the elastic lithosphere. We think that the elastic assumption is acceptable for the following reason. The principle strains in our numerical models are mostly less than 1% and few are 1∼2.5%. The maximum shortening or elongation of sandstone is up to 2.5% when the axial differential stress $\sigma_1-\sigma_3$ is less than failure strength under the confining pressure of 50 MPa as shown in Fig. 10 (Hoshino et al., 1972).

The simulated result of model S, in which the spreading displacement of 80 m and the convergence displacement varying from 504 m to 168 m are subjected as the boundary condition, is in agreement with the earthquake focal mechanism in the Okinawa Trough. From the focal mechanism, stress is tensional in the trough as illustrated in Fig. 4 (Shiono et al., 1980). The simulated stress field of model S shows that σ_3 is tensional in the trough (Fig. 8). The simulated result of model S also coincides with the earthquake focal mechanism within the accretionary prism of the Eurasia plate. According to the focal mechanism, thrust faults develop within the accretionary prism as shown in Fig. 4 (Shiono et al., 1980). The simulated result also shows that there are some finite elements with $P_f>1.0$ within the accretionary prism in model S, where thrust faults develop (Fig. 9).

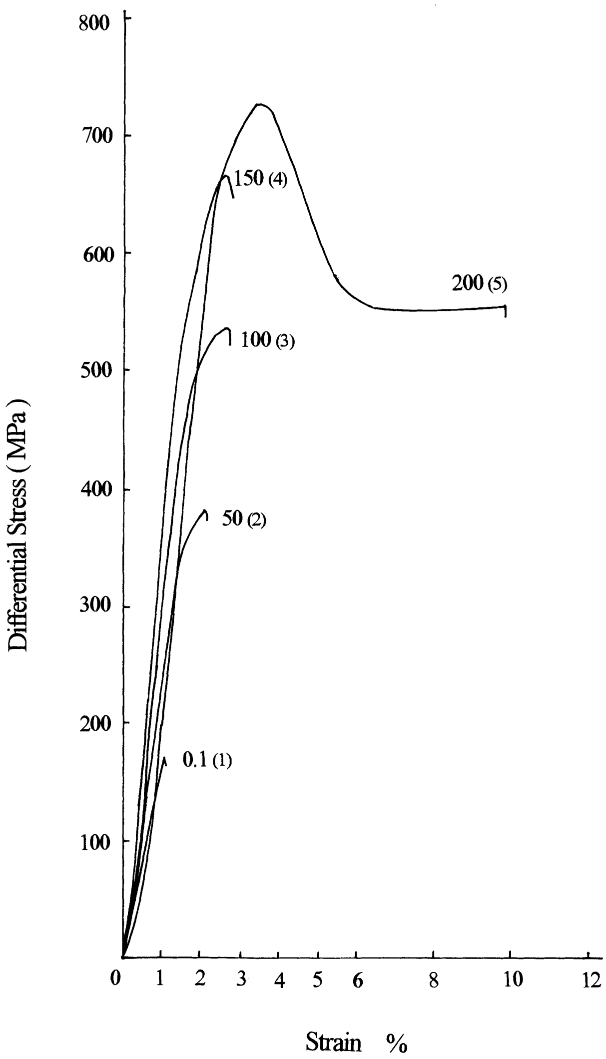

Fig. 10 Stress-strain curve for Furukawa sandstone, HSF (S98) after Hoshino et al. (1972).

The spreading of the Okinawa Trough is simplified as the spreading displacement along the crust bottom. As the PHS plate subducts beneath the Eurasia plate, the convergence litho-

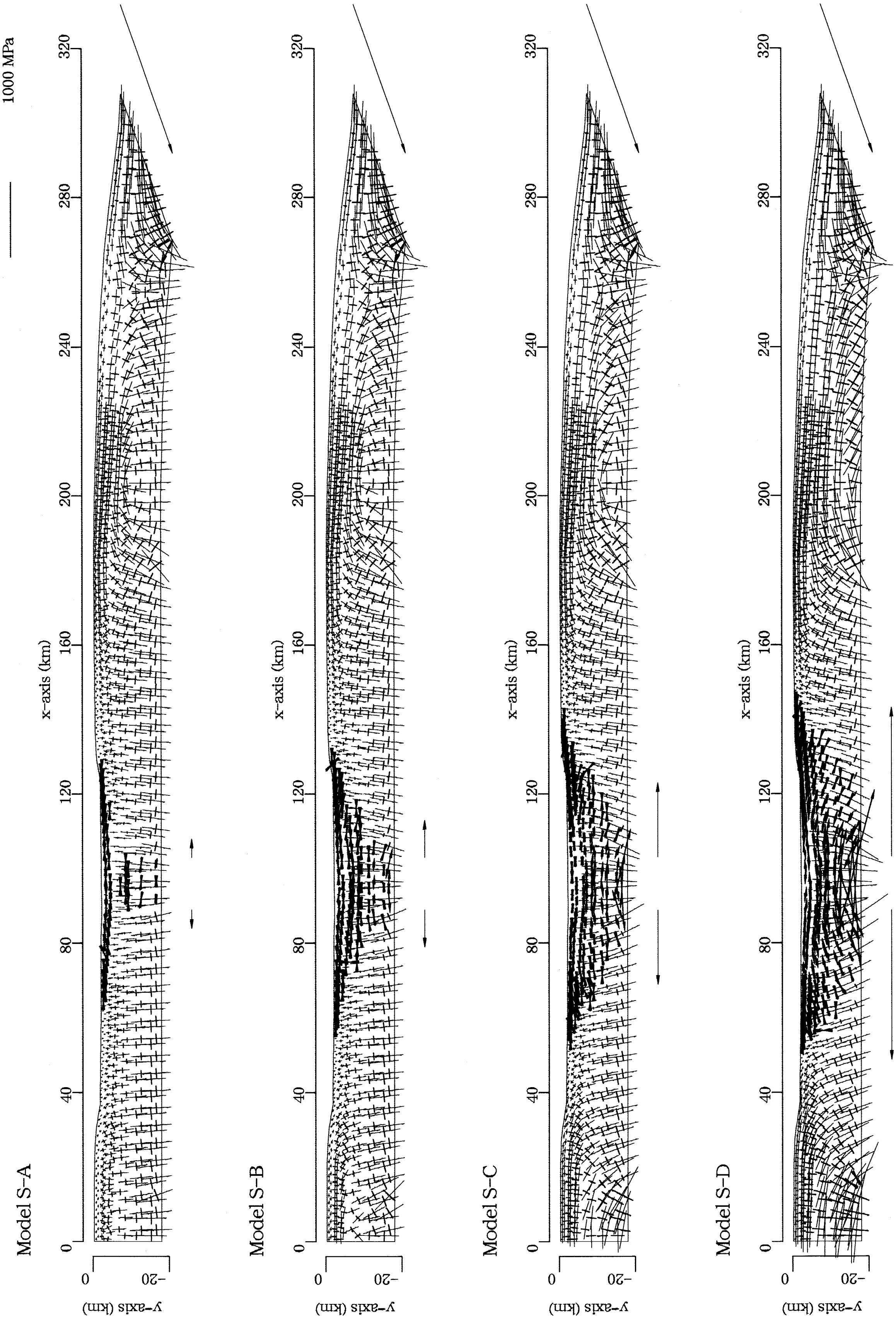

Fig. 11 Magnitude and orientation of the principal stresses in the semi-3D stress fields of models S-A, S-B, S-C and S-D. The value of the spreading displacement varies in the four models while the values of the convergence displacement are fixed.

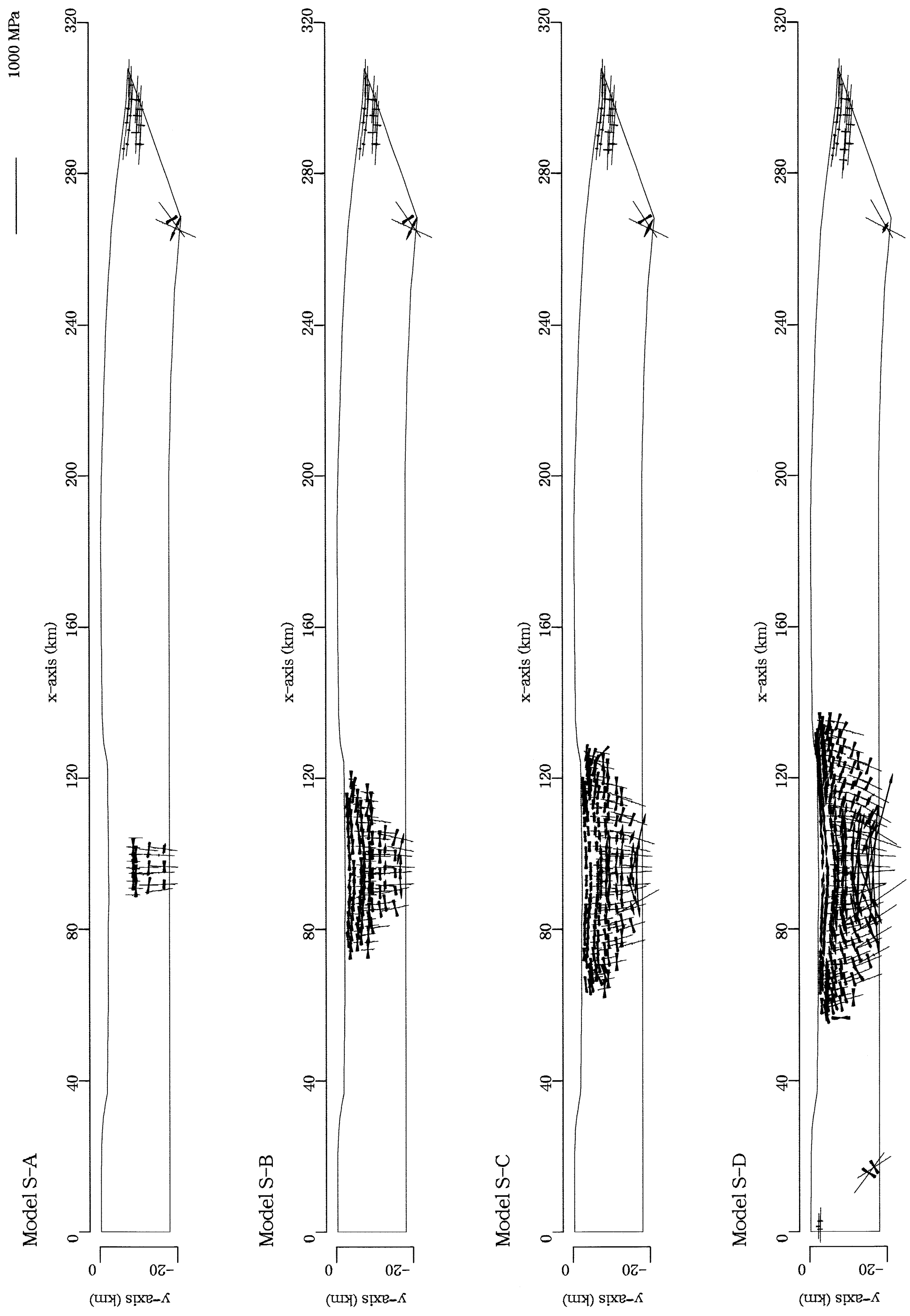

Fig. 12 Fault development in models S-A, S-B, S-C and S-D. The maximum and minimum principal stresses are illustrated just for the finite element with Pf>1.0 in the four models. Note that the intensity of the spreading displacement regulates the development of normal fault in the trough.

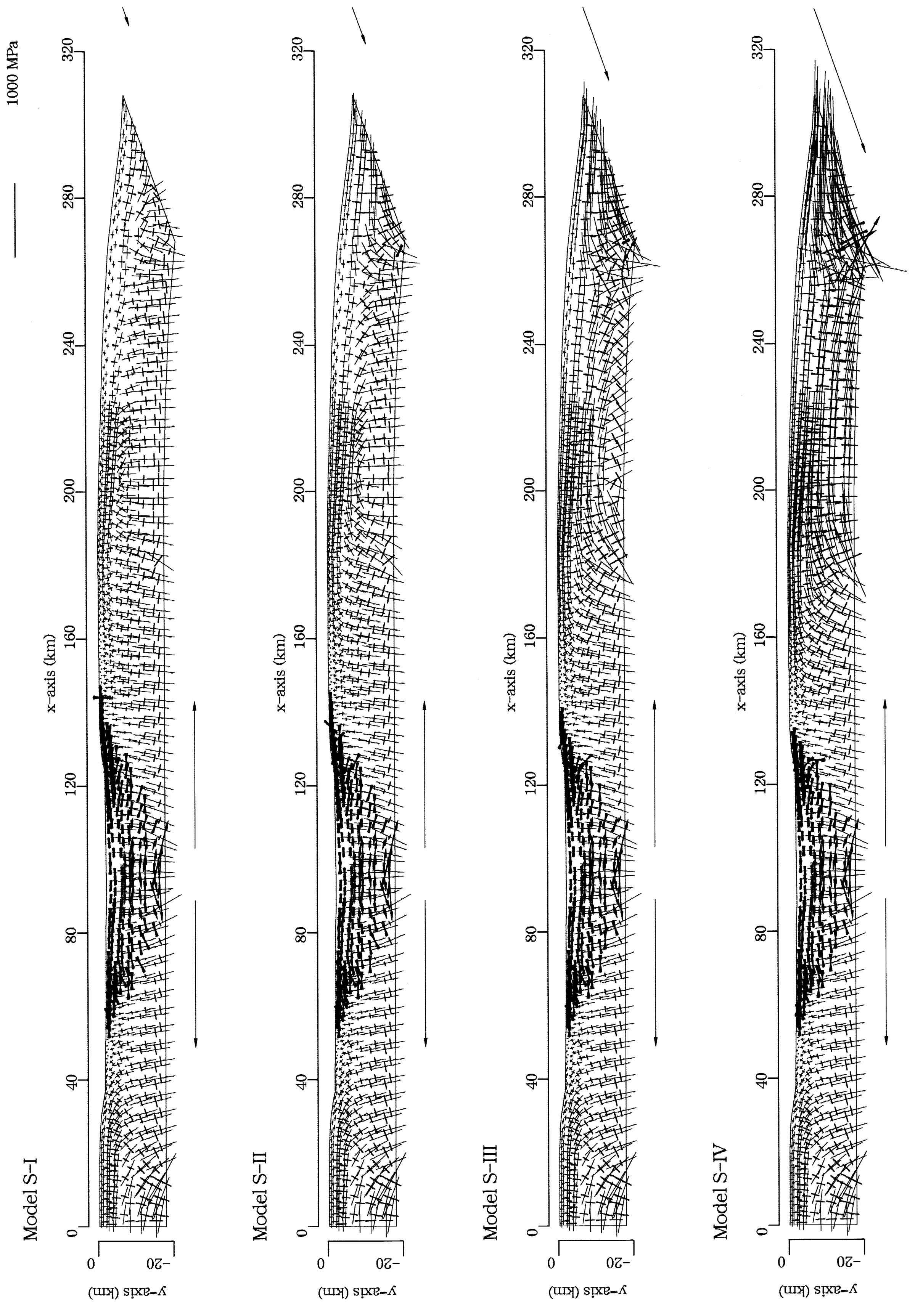

Fig. 13 Magnitude and orientation of the principal stresses in the semi-3D stress fields of models S-I, S-II, S-III and S-IV. The value of the spreading displacement is fixed while the values of the convergence displacement vary in the four models.

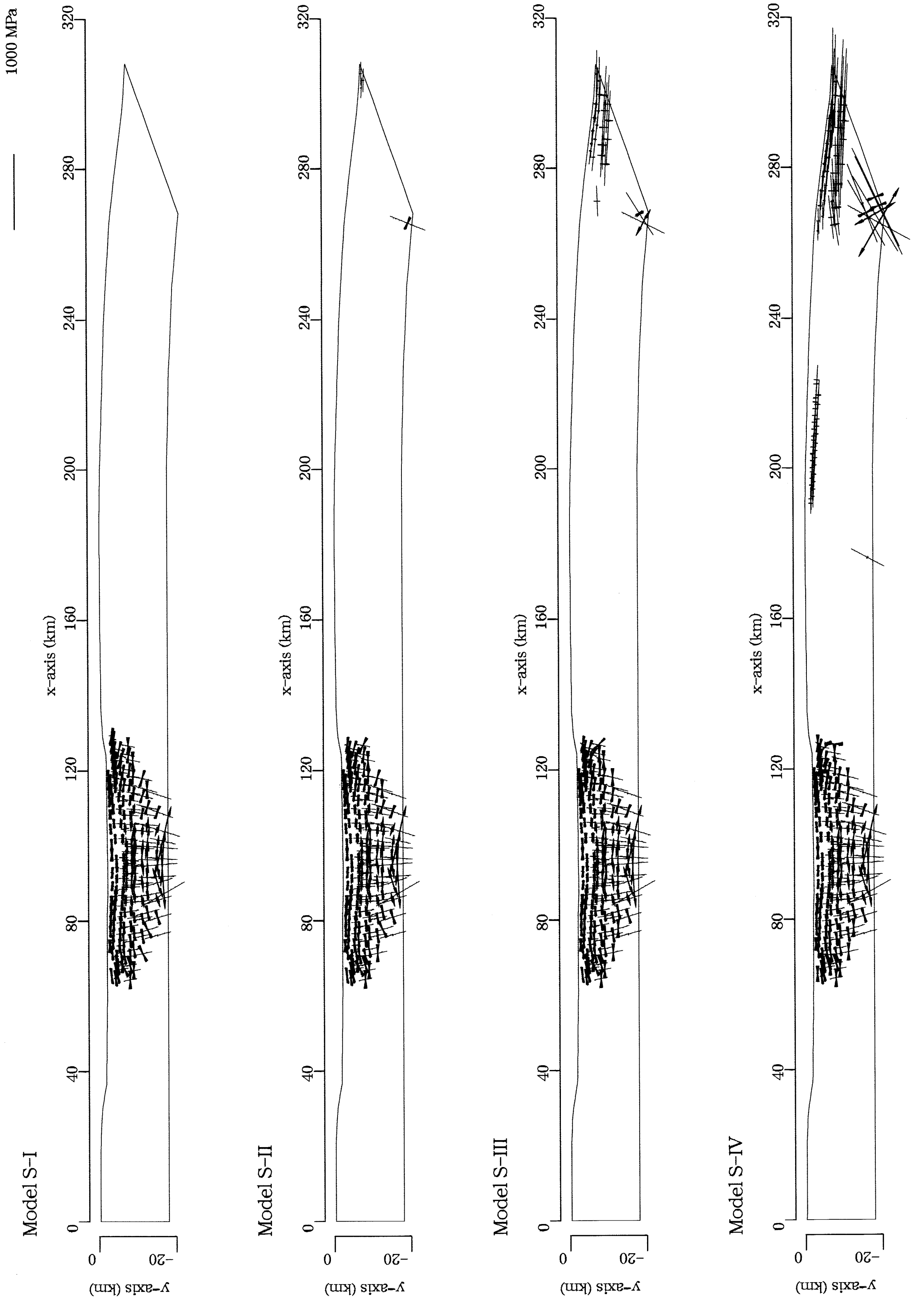

Fig. 14 Fault development in models S-I, S-II, S-III and S-IV. The maximum and minimum principal stresses are illustrated just for the finite element with Pf > 1.0 in the four models. Note that the intensity of the convergence displacement controls the thrust development within the accretionary prism of the Eurasia plate.

sphere induces a secondary convection cell (Turcotte and Schubert, 1982). The positive and negative values of the spreading displacement indicate the two different directions of the mantle convection under the trough. This is the significance of the spreading displacement under the trough in numerical models.

The convergence displacement is applied along the subduction slope in finite element models. The application of the varying convergence displacement is somewhat arbitrary. To get a similar simulated results with the earthquake focal mechanism (Shiono et al., 1980), the varying convergence displacement is applied along the subduction slope and thrust faults develop within the accretionary prism. On the other hand no thrust development occurs as the constant convergence displacement is imposed along the subduction slope. More detailed discussion about the varying convergence displacement or the slip deficiency along the subduction slope is beyond the scope of this paper.

Although the role of the two types of displacement boundary condition to the fault development is shown up, the influence of the intensity of the spreading and convergence displacements is unknown. In order to make out the influence of the intensity of the spreading displacement to the development of normal fault in the Okinawa Trough, stress fields of models S-A, S-B, S-C and S-D are simulated (Fig. 11). The spreading displacement varies in the four models while the convergence displacements are fixed (Table 2). The finite-element grid of the four models is the same as model S.

The stress fields of models S-A, S-B, S-C and S-D show different features from each other. In the trough, tensional σ_3 becomes stronger and occupies more extensive area as the value of the spreading displacement increases. Within the accretionary prism of the Eurasia plate, the stress distributions of the four models are similar to each other. Thus the intensity of the spreading displacement decides the magnitude and area of tensional stress in the Okinawa Trough.

The development style of normal fault in the trough is different in models S-A, S-B, S-C and S-D as illustrated in Fig. 12. In the trough, normal faults develop at the deep place in model S-A, and develop within more extensive area in model S-B. As the value of the spreading displacement increases, normal faults develop within almost all the finite elements in the trough. However within the accretionary prism of the Eurasia plate, thrust development is similar in the four models. Thus the intensity of the spreading displacement controls the occurrence and area of normal fault in the Okinawa Trough.

In order to know the influence of the intensity of the convergence displacement to the thrust development within the acretionary prism of the Eurasia plate, stress fields of models S-I, S-II, S-III and S-IV are simulated (Fig. 13). The value of the spreading displacement is unchanged in the four models while the values of the convergence displacement are varied (Table 2). The finite-element grid of the four models is the same as model S.

The stress fields of models S-I, S-II, S-III and S-IV show different features from each other. Within the accretionary prism, compressive σ_1 tends to be nearly horizontal, and increases its area from the shallow to deep place as the values of the convergence displacement increase. However, in the trough, the stress distribution is similar in the four models. Thus the intensity of the convergence displacement changes the orientation and area of horizontal compressive σ_1 within the accretionary prism of the Eurasia plate.

The style of thrust development within the accretionary prism is different in models S-I, S-II, S-III and S-IV as shown in Fig. 14. No thrust fault develops in model S-I. There are few finite elements with $P_f > 1.0$ at the shallow place within the accretionary prism in model S-II, where thrust faults develop. As the values of the convergence displacement increase, thrust faults develop within almost the whole accretionary prism. However the development of nomal fault in the trough is similar in the four models. Thus the intensity of the convergence displacement regulates the occurrence and area of thrust faults within the accretionary prism of the Eurasia plate.

Conclusions

In this paper, semi-3D stress fields of the Eurasia plate are simulated with a series of finite element models. The spreading displacement along the crustal bottom under the Okinawa Trough and/or the convergence displacement attached along the upper side of the PHS plate are subjected as the boundary condition. The development style of normal fault in the back-arc trough and thrust fault within the accretionary prism of the Eurasia plate is analyzed. The results obtained from the numerical experiment allow us to draw the following conclusions.

The spreading displacement under the trough is one type of displacement boundary condition for numerical model. Tensional stress appears and normal faults develop in the trough as the spreading displacement is applied as the boundary condition. On the other hand there is no tension and no normal fault develops in the trough with zero spreading displacement subjected. The spreading displacement along the crustal bottom beneath the trough raises up tensional stress and generates normal faults in the trough. The intensity of the spreading displacement controls the area of tensional stress and normal fault in the trough. However the convergence displacement has little effect on the stress distribution and development style of normal fault in the trough. Since normal faults in a tensional terrane often leads to the formation of a trough structure (Melosh & Williams, 1989), the genesis of the Okinawa Trough is the spreading along the crustal bottom beneath the back-arc trough.

The convergence displacement attached along the upper side of the PHS plate is the other type of displacement boundary condition for numerical model. Thrust faults develop within the accretionary prism of the Eurasia plate as the convergence displacement is loaded. However no thrust fault develops with zero convergence displacement subjected. The convergence displacement causes thrust development within the accretionary prism. The intensity of the convergence displacement controls the area of thrust fault within the accretionary prism, but the spreading displacement hardly affects the stress distribution and style of thrust development within the accretionary prism of the Eurasia plate. The genesis of the thrust development within the accretionary prism is the subduction of the PHS plate beneath the Eurasia plate.

Acknowledgements

H. Lu would like to express his appreciation to Ministry of Education, Culture, Sports, Science and Technology and Association of International Education, Japan for the financial support of scholarship to this work.

References

Clark, S.P., 1966, Handbook of Physical Constants. The Geological Society of America, *INC.*, reversed ed., 587 p.

Hayashi, D. and Kizaki, K., 1972, Numerical analysis on migmatite dome with special reference to finite element method. *J. Geol. Soc. Japan* **78** (12), 677–686.

Herman, B.M., Anderson, R.N. and Truchan, M., 1979. Extensional tectonics in the Okinawa Trough. *In* Watkins, J.S., Montadert, L., Dickinson, P.W., ed., *Geological and Geophysical Investigations of Continental Margins.* American Association of Petroleum Geologists Memoir 29, Tulsa, Oklahoma, pp. 199–208.

Hirata, N., Kinoshita, H., Katao, H., Baba, H., Kaiho, Y., Koresawa, S., Ono, Y. and Hayashi, K., 1991. Report on DELP 1988 Cruises in the Okinawa Trough : Part 3. Crustal Structure of the Southern Okinawa Trough. *Bull. Earthquake Res. Inst., Univ. Tokyo* **66**, 37–70.

Hoshino, K., Koide, H., Inami, K., Iwamura, S. and Mitsui, S., 1972. Mechanical Properties of Japanese Tertiary Sedimentary Rocks under High Confining Pressures. *Geological Survey of Japan Report,* no. 244. Geological Survey of Japan, Tokyo, 200 p.

Huchon, P., Barrier, E., De Bremaecker, J.C. and Angelier, J., 1986, Collision and stress trajectories in Taiwan : a finite element model. *Tectonophysics,* **125**, 179–191.

Iwasaki, T., Hirata, N., Kanazawa, T., Melles, J., Suyehiro, K., Urabe, T., Moller, L., Makris, J. and Shimamura, H., 1990, Crustal and upper mantle structure in the Ryukyu Island Arc deduced from deep seismic sounding. *Geophys. J. Int.,* **102**, 631–651.

Hu, J.C., Angelier, J., Lee, J.C., Chu, H.T. and Byrne, D., 1996, Kinematics of convergence, deformation and stress distribution in the Taiwan collision area : 2-D finite-element numerical modelling. *Tectonophysics,* **255**, 243–268.

Kimura, M., 1983, Formation of the Okinawa Trough graben (in Japanese with English abstract). The memoirs of the Geological Society of Japan, no. 22. Geological Society of Japan, Tokyo, pp. 141–157.

Kimura, M., 1985, Back-arc rifting in the Okinawa Trough. *Mar. Pet. Geol.,* **2**, 221–240.

Kobayashi, K., 1985, Sea of Japan and Okinawa Trough. *In* Nairn, A. E. M., Stehli, F. G., Uyeda, S., eds., *The Ocean Basins and Margins,* Vol. 7A. Plenum, New York, pp. 419–458.

Kodaira, S., Iwasaki, T., Urabe, T., Kanazawa, T., Egloff, F., Makris, J. and Shimamura, H., 1996, Crustal structure across the middle Ryukyu trench obtained from ocean bottom seismographic data. *Tectonophysics* **263**, 39–60.

Lee, C. S., Shor, G. G., Bibee, L. D., Lu, R. S. and Hilde, T. W. C., 1980, Okinawa Trough : origin of a back-arc basin. *Mar. Geol.,* **35**, 219–41.

Letouzey, J. and Kimura, M., 1985. Okinawa Trough genesis : structure and evolution of a back-arc basin developed in a continent. *Mar. Pet. Geol.,* **2**, 111–130.

Letouzey, J. and Kimura, M., 1986, The Okinawa Trough : genesis of a back-arc basin developing along a continental margin. *Tectonophysics,* **125**, 209–230.

Ludwing, W. J., Murauchi, S., Den, N., Buhl, P., Hotta, H., Ewing, M., Asanuma, T., Yoshii, T. and Sakajiri, N., 1973, Structure of East China Sea-West Philippine Sea Margin off Southern Kyushu, Japan. *J. Geophys. Res.,* **78**, 2,526–2,536.

Lu, H., 1998. Two dimensional stress analysis in profiles of Ryukyu Trench-Ryukyu Arc-Okinawa Trough with special reference to finite element method. Unpublished Master thesis, Graduate School of Science, University of the Ryukyus, Okinawa.

Melosh, H. J. and Williams, C. A., 1989, Mechanics of Graben Formation in Crustal Rocks : A Finite Element Analysis. *J. Geophys. Res.,* **94**, 13,961–13,973.

Miki, M., 1995. Two-phase opening model for the Okinawa Trough inferred from paleomagnetic study of the Ryukyu arc. *J. Geophys. Res.* **100**, 8,169–8,184.

Nagumo, S., Kinoshita, H., Kasahara, J., Ouchi, T., Takuyama, H., Asamuma, T., Koresawa, S. and Akiyoshi, H., 1986. Report on DELP 1984 Cruise in the middle Okinawa Trough, Part II : Seismic Structural Studies. *Bull. Earthquake Res. Inst. University of Tokyo,* **61**, 167–202.

Park, J. O., Tokuyama, H., Shinohara, M., Suyehiro, K. and Taira, A., 1998, Seismic record of tectonic evolution and backarc rifting in the southern Ryukyu island arc system. *Tectonophysics* **294**, 21–42.

Sato, T. and Matsuura, M., 1993. A kinematic model for evolution of island arc-trench systems. *Geophys. J. Int.* **114**, 512–530.

Seno, T., 1977, The Instantaneous Rotation Vector of the Philippine Sea plate Relative to the Eurasian Plate. *Tectonophysics* **42**, 209–26.

Shiono, K., Mikumo, T. and Ishikawa, Y., 1980, Tectonics of the Kyusyu-Ryukyu Arc as evidenced from seismicity and focal mechanism of shallow to intermediate-depth earthquakes. *J. Phys. Earth,* **28**, 17–43.

Sibuet, J. C., Letouzey, J., Barbier, F., Charvet, J., Foucher, J. P., Hilde, T. W. C., Kimura, M., Chiao, L. Y., Marsset, B., Muller, C. and Stephan, J. F., 1987, Back arc extension in the Okinawa Trough. *J. Geophys. Res.* **92**, 14,041–14,063.

Sibuet, J. C., Deffontaines, B., Hsu, S. K., Thareau, N., Formal, J. P. L., Liu, C. S. and ACT party, 1998, Okinawa trough backarc basin : Early tectonic and magmatic evolution. *J. Geophys. Res.* **103**, 30,245–30,267.

Timoshenko, S. P. and Goodier, J. N., 1970, Theory of Elasticity. McGraw-Hill, London, 3rd ed., 567 p.

Turcotte, D. L. and Schubert, G., 1982, Geodynamics-Applications of Continuum Physics to Geological Problems. John Wiley & Sons, New York, 450 p.

Viallon, C., Huchon, P. and Barrier, E., 1986, Opening of the Okinawa basin and collision in Taiwan : a retreating trench model with lateral anchoring. *Earth Planet. Sci. Lett.,* **80**, 145–155.

Wageman, J. M., Hilde, T. W. C. and Emery, K. O., 1970, Structural framework of East China Sea and Yellow Sea. *The American Association of Petroleum Geologists Bulletin,* **54**, 1,611–1,643.